Biogeochemistry of Household Dust Samples Collected from Private Homes of a Portuguese Industrial City

Amélia P. Marinho-Reis [1,2,*], Cristiana Costa [2], Fernando Rocha [2], Mark Cave [3], Joanna Wragg [3], Teresa Valente [1], Amália Sequeira-Braga [1] and Yves Noack [4]

[1] Departamento de Ciências da Terra, Instituto de Ciências da Terra, Campus de Gualtar, Polo da Universidade do Minho, 4710-057 Braga, Portugal; teresav@dct.uminho.pt (T.V.); masbraga@dct.uminho.pt (A.S.-B.)

[2] Departmento de Geociências, GEOBIOTEC, Campus Universitário de Santiago, Universidade de Aveiro, 3810-193 Aveiro, Portugal; tavares.rocha@ua.pt (F.R.); cristianacosta@ua.pt (C.C.)

[3] British Geological Survey, Keyworth, Nottingham NG12 5GG, UK; jwrag@bgs.ac.uk (J.W.); mrca@bgs.ac.uk (M.C.)

[4] CNRS, IRD, INRAE, Collège de France, Aix-Marseille Univ., CEREGE, BP 80, 13545 Aix en Provence, France; nozck@cerege.fr

* Correspondence: pmarinho@dct.uminho.pt

Abstract: The main objectives of the present study were to (i) investigate the effects of mineralogy and solid-phase distribution on element bioaccessibility and (ii) perform a risk assessment to calculate the risks to human health via the ingestion pathway. Multiple discriminant analysis showed that the dust chemistry discriminates between indoor and outdoor samples. The solid-phase distribution of the elements in indoor dust indicated that a large proportion of zinc, nickel, lead, copper, and cobalt is associated with an aluminum oxy-hydroxides component, formed by the weathering of aluminum silicates. This component, which seems to influence the mobility of many trace elements, was identified for a group of indoor dust samples that probably had a considerable contribution from outdoor dust. An iron oxide component consisted of the highest percentage of chromium, arsenic, antimony, and tin, indicating low mobility for these elements. The bioaccessible fraction in the stomach phase from the unified BARGE method was generally high in zinc, cadmium, and lead and low in nickel, cobalt, copper, chromium, and antimony. Unlike other potentially toxic elements, copper and nickel associated with aluminum oxy-hydroxides and calcium carbonates were not extracted by the stomach solutions. These trace elements possibly form stable complexes with gastric fluid constituents such as pepsin and amino acid. Lead had a hazard quotient >1, which indicates the risk of non-carcinogenic health effects, especially for children.

Keywords: potentially toxic elements; oral bioaccessibility; solid-phase distribution; human exposure; risk assessment

1. Introduction

We typically spend over 80% of the day inside, yet our indoor environments are still poorly understood. Household air pollution results in an estimated 3.8 million premature deaths globally each year [1], representing a significant public health challenge. The home environment can be a source of passive or active exposure to environmental contaminants such as persistent organic contaminants, metals and metalloids, minerals, allergens, hair, ash, soot, cooking and heating residues, tobacco smoke, and building components, among others. While a large body of literature is devoted to suspended particulate matter (PM) in the indoor environment [2–10], to date, fewer studies have focused on the

characterization of indoor dust settled on the floor from homes [11–14], which is commonly designated as household dust. However, the involuntary ingestion of household dust is a significant non-dietary pathway for hazardous substances such as metals and metalloids, potentially leading to undesired health effects, especially for children. Children are typically more susceptible to the impacts of acute and chronic environmental contaminant exposures because they are exposed to indoor dust accumulated on floors and other surfaces. Further, infants and children typically engage in more hand-to-mouth activity than other age groups, which might involve the placement of toys contaminated with dust in their mouth or the consumption of food with contaminated fingers [15]. There is, therefore, a necessity to identify and characterize the hazards associated with indoor dust to develop ways of reducing the associated risks and make our homes safer.

Dust chemical/mineralogical composition is very variable and depends heavily on pathways and modes of introduction of pollutants into an indoor environment [16]. Minerals such as quartz and asbestos have toxic features that, despite numerous experimental studies in the field, their mechanisms of toxicity have not yet been fully clarified [17]. Therefore, a detailed knowledge of what makes a mineral particle toxic is urgently needed not only to understand the cause of well-known diseases but also to predict which minerals might be dangerous.

No studies were found that have considered human contact with potentially toxic elements (PTEs) in household dust in the Portuguese context. Most human exposure assessment estimates have been based on exposure to soil and outdoor dust [18,19]. Indoor dust is thus a common but overlooked exposure pathway for PTEs in Portuguese homes.

Most exposure and health risk assessment studies seem to agree that oral ingestion is the primary exposure route to PTEs for humans, compared with inhalation and dermal contact [20–22]. Although many studies have demonstrated the importance of oral bioaccessibility in assessing human health risks from the soil, there is a scarcity of research on the oral bioaccessibility of PTEs in household dust for risk assessment purposes. Hence, the objectives of the present study were to: (1) characterize the chemical composition of the household dust; (2) estimate the PTE bioaccessible geochemical sources in the indoor dust; (3) investigate the effects of mineralogy and solid-phase distribution on the in vitro PTE bioaccessibility; and (4) perform a risk assessment to calculate risks to human health via the ingestion pathway for two age groups.

2. Materials and Methods

2.1. The Study Area

Estarreja is a coastal municipality on the North-western Portuguese coast that extends over an area of 108.2 km^2 and has an estimated resident population of 26,242 inhabitants. The majority of the land is used for agriculture (54%), while 27% is forest land and 18% include urban and peri-urban areas [23]. The location of both the municipality and the study area, within the Portuguese territory, are provided as Supplementary Information (Figure S1).

Due to its geography, it is part of the temperate climates (type Csb according to the Köppen–Geiger climate classification system) with a Mediterranean influence.

The geology is characterized mainly by Quaternary unconsolidated sands and clays deposited on dune, beach, and lagoon environments. These sedimentary units, generally a dozen meters thick, dip gently to the west, overlying Proterozoic metamorphic rocks and Mesozoic siliciclastic formations [24].

One of the most important industrial complexes of the country since the 1950s, known as the chemical complex of Estarreja (CCE), is located close to the small urban center of Estarreja (Figure S1). The industrial facilities include heavy industry, which has been described in detail elsewhere [25]. These complexes have produced a variety of organic and inorganic compounds such as nitric acid, aniline, nitrobenzene, sodium, and chlorate compounds from rock salt, synthetic resins, and polyurethanes. In the past, the liquid effluents discharged by these industries contained large amounts of hazardous substances such as aniline, nitrobenzene, arsenic (As), mercury (Hg), zinc (Zn), and lead (Pb),

among others. Although technological upgrades associated with remediation measures have been implemented by the industry over recent decades and have successfully reduced the environmental burden, the CCE continues to be held the most significant polluter of the region.

2.2. Household Dust Sampling

Nineteen homes located close to the industrial facilities were selected for the study. Although the majority was in urban to peri-urban areas, some of the houses were in rural settings (Figure S1).

In this study, the term household dust encompasses both dust samples collected from indoor and outdoor areas of the house (hereafter identified as indoor dust and outdoor dust, respectively). Aiming to assess potential differences in dust geochemistry and mineralogy, indoor and paired outdoor dust samples were collected from the households. Information from both settings has the potential to increase our understanding of sources, mobility, and the fate of the PTEs in the home environment. The outdoor dust was collected from areas as patios, garden paths, and driveways, using a small dustpan and brush. A composite indoor dust sample was collected from different rooms using a vacuum sampler as described elsewhere [26]. The <150 μm particle size fraction of the house dust was obtained by dry sieving [26].

2.3. Instrumentation

The mineral composition of indoor and paired outdoor dust samples was determined via X-ray diffraction (XRD) analysis using a PhilipsX'Pert MPD (Marvel Panalytical, Almelo, The Netherlands), equipped with an automatic divergence slit, a CuKa (λ = 1.5405) radiation (20 mA and 40 kV), and a Ni filter. X'Pert HighScore Plus©2006 PANalytical B.V. (v.2.2) (Marvel Panalytical, Almelo, The Netherlands) software was used, supported by the database of the International Center for Diffraction Data (ICDD) for the diffractogram interpretation phase. The first step was mineral identification, and then the peaks of each mineral were scaled manually to give the best fit to the observed XRD diffractogram. The bulk mineralogy was determined in random powders. Semi-quantitative estimation in the bulk rock was obtained by the relative intensity of diagnostic reflection of each mineral in the XRD patterns. The mineral composition obtained using this semi-quantitative approach is known to be very useful for comparisons between samples [27,28].

All chemicals used were of certified analytical grade. Dust samples were digested with aqua regia at 90 °C in a microprocessor-controlled digestion block for 2 h, and the analysis of 37 chemical elements was carried out by inductively coupled plasma-mass spectrometry (ICP-MS) at ACTLABS Analytical Laboratory, Canada. Each sample batch prepared for ICP-MS analysis included dust samples, duplicates, blanks, and standard reference materials, for quality assurance and quality control (QC/QA) procedures. The Certified Reference Materials GRX-1, GRX-4, GRX- 6, and SAR-M (United States Geological Survey) were selected to represent a wide range of total elemental concentrations. Results of method blanks were always below detection limits. Values for precision, expressed as RSD %, were typically less than 15% for all elements.

Following the chemical-mineralogical characterization, nine indoor dust samples were selected for bioaccessibility testing. The oral bioaccessibility of the PTE was determined using the unified BARGE method (UBM) (ISO 17924:2018) [29]. The concentrations of 16 chemical elements were analysed in the UBM extracts by ICP-MS at CEREGE, France. For quality control purposes, duplicate samples, blanks, and the bioaccessibility guidance material BGS 102 were extracted with every batch of the UBM extractions. The blanks always returned results that were below the detection limit.

Indoor dust is a complex mixture of organic and inorganic particles that have settled onto objects, surfaces, floors, and carpeting and acts as a reservoir of PTEs. The occurrence and relative distribution of PTE among the different components of the dust controls their dissolution and hence bioaccessibility [30,31]. To assess the distribution of the trace elements amongst the different dust components, a multi-step sequential extraction method known as CISED (CISED stands for the Chemometric Identification of Substrates and Element Distributions) was employed to identify

geochemically distinct components extracted by increasing concentrations of aqua regia [32]. A total of four indoor dust samples (<150 µm fraction) were extracted using the CISED extraction method. The small amount of dust available for most sites, after several rounds of chemical analysis, justifies the small number of samples used to perform the solid-phase distribution study. Seven solutions, covering the extraction concentration range deionized (DI) water to 5.0 M acid, were used in duplicate, with progressive addition of H_2O_2 (0.25, 0.50, 0.75, and 1 mL) in the last four extracting solutions to facilitate the precipitation of oxides [33]. A total of 14 extracts per dust were obtained for analysis of 30 elements by ICP-MS. Subsequently, the multi-element extract data were subject to a chemometric self-modelling mixture resolution (SMMR) procedure, as described elsewhere [32,34]. For data quality control, blanks, and reference material (BGS102) were included in the extraction procedure. An earlier version of this same reference material has been analysed previously by Cave and co-authors [35]. Several studies were shown the CISED as a useful methodology for understanding the biogeochemistry of trace elements in soil and dust [30,34,36].

2.4. Statistical Techniques

Univariate and bivariate statistics, distribution plots, and scatterplots were examined for all variables. Boxplots and the Shapiro-Wilk test were used to check whether the variables under study had a normal distribution. The results indicated that most variables were not normally distributed, within a 95% significance level. When normal distribution could not be accepted, variable transformations (square, square root, and logarithmic) were attempted. The base-10 logarithm and the square root transformations helped to improve the distribution shape. Spearman's rank correlation coefficients (Spearman's rho) were calculated to identify relationships between indoor and outdoor dust chemical concentrations. Differences between groups were tested using the Mann–Whitney U test. A probability of 0.05 or lower was regarded as significant in testing the null hypothesis of no differences in concentration between indoor and outdoor dust samples.

Discriminant analysis was applied to dust chemistry data to identify those chemical elements providing the best separation between indoor and outdoor dust. Multiple discriminant analysis (MDA) is a multivariate technique of data analysis used to determine how well two or more groups of samples can be classified into pre-defined groups based on a particular characteristic. In this study, the characteristic of interest was the chemical composition of the household dust samples. MDA estimates discriminant functions that are linear combinations of the data by maximizing the ratio of the between-group variance and the within-group variance. These functions are then used to assess differences between groups or to classify samples into groups. The method has been used widely, mainly to classify environmental samples based on known sources [37–39]. The number of discriminant functions estimated is one less than the number of groups being classified [40]. For the analysis of the two groups, outdoor dust (OUT) and indoor dust (IN), one discriminant function was estimated. The MDA model classifies each sample into a group by calculating the distance between sample's canonical discriminant score and the centroid canonical discriminant score for each of the groups and choosing the group whose centroid is closest to the sample score. A good MDA model should have a low misclassification rate that is significantly different from the classification that might occur by chance [38].

Univariate and bivariate statistics, boxplots, the Shapiro-Wilk and the Mann-Whitney U tests, and MDA analysis were performed using the IBM SPSS (v. 21) software.

2.5. Exposure and Risk Assessment

In the developed strategy, exposure was calculated according to a scenario evaluation approach that uses data on chemical concentration, frequency, and duration of exposure as well as information on the behaviors and characteristics of the exposed receptor at a given life stage [41]. The scenario considered was the average amount of time children (6 to 17 years old) and adults (<75 years old)

spend indoor in the home environment [41], as this was considered the most appropriate for our case study.

For many non-cancer effects, the potential exposure to contaminated soil/dust was expressed in the form of the average daily dose (ADD) according to the following equation [42]:

$$\text{ADD} = C_{\text{dust}} \times \frac{\text{IR} \times \text{EF} \times \text{ED} \times 10^{-6}}{\text{BW} \times \text{AT}}. \tag{1}$$

C = concentration (mg kg^{-1}), IR = intake rate (mg kg^{-1}), ED = exposure duration (years), EF = exposure frequency (days year^{-1}) and AT = averaging time (days). C in Equation (1) was expressed as an estimate of the arithmetic mean regardless of the distribution of the data [42]. The ED corresponded to the median age for each age group (children: 11.5; adults: 46.5), and the IR used was 60 mg day^{-1} for children and 30 mg day^{-1} for adults, which are estimates for indoor dust only [41]. The EF considered corresponds to the mean of the total amount of time spent indoors at residence (min day^{-1}): 833 for children and 948 for adults. The 10^{-6} factor is the unit conversion factor. For non-chronic non-cancer effects, the time period (AT) was the averaged exposure time (ED × 365 days). By averaging across different age groups, the following values were obtained for body weight (BW): 70 kg for adults and 53.4 kg for children [41].

Given that site-specific bioaccessibility values were available, the exposure estimate was adjusted by calculating the hazard quotient (HQ) [42]:

$$\text{HQ} = \frac{\text{ADD} \times \text{BAF in \%}}{\text{RfD}}. \tag{2}$$

To calculate the HQ, an oral reference dose (RfD) is necessary. However, the U.S. EPA has not established an RfD for cobalt (Co), copper (Cu), and Pb. Nevertheless, it can be derived from the no observed adverse effect level (NOAEL), with uncertainty factors generally applied to reflect limitations of the data used [43]. Hence, the oral reference doses used in this study were 0.0003, 0.01, and 0.002 mg kg^{-1} day^{-1} for Co [44], Cu [45], and Pb [43], respectively. The Integrated Risk Information System (IRIS) of the U.S. EPA has the oral reference dose for antimony (Sb), cadmium (Cd), chromium (Cr), nickel (Ni), and Zn, at 0.0004, 0.001, 0.003, 0.02, and 0.3 mg kg^{-1} day^{-1}, respectively. The value used for the bioaccessible fraction (BAF) (% bioaccessibility) corresponded to the average concentration extracted by the UBM stomach solutions from nine indoor dust samples.

The hazard index (HI) was the sum of the individual target hazard quotients of the elements assessed. Even if individual HQs for the PTEs in the indoor dust are lower than unity individually, the cumulative effect of incidental ingestion may result in adverse health effects [43]. If the HI is >1 there is the potential for adverse non-carcinogenic health effects. The equation for HI is:

$$\text{HI} = \sum_{n=1}^{i} \text{HQ}_n. \tag{3}$$

3. Results and Discussion

3.1. Mineralogy of the Household Dust Samples

The mineralogical study performed by XRD indicated that both indoor and outdoor samples are primarily composed of high crystallinity minerals, namely quartz, and calcite (Table 1).

Table 1. Average mineralogical composition in % estimated by XRD (major high-crystallinity phases). Key: Q—quartz; F—K-feldspar; P—plagioclase; Mi—mica; Ca—calcite.

House Dust	N	Q	F	P	Mi	Ca
INDOOR	15	28	14	15	3	37
OUTDOOR	17	37	17	19	8	17

High crystallinity phases such as quartz, potassium (K)-feldspar, plagioclase, and mica usually occurred in higher average concentrations in outdoor samples, which is in agreement with the expected outdoor predominance of geogenic materials, namely from soil particles. Calcite showed a different trend as it was enriched in the indoor samples relative to the outdoor dust. Besides mineral soil particles tracked indoors on the soles of our shoes, building components such as concrete, plaster, or tile debris are likely sources of calcite found in the home environment. Minor mineral phases include brucite $Mg(OH)_2$, berthiérine, chrysolite, lizardite, goethite, lepidocrocite $FeO(OH)$, and gibbsite $Al(OH)_3$. Therefore, the set of identified minerals included a variety of minerals with different morphological features. Planar and fibrous serpentine (lizardite and chrysotile, respectively), 7 Å chlorite (berthiérine), as well as oxy-hydroxides of magnesium (Mg), aluminum (Al), and iron (Fe) that are usually associated with the weathering of Mg-silicates such as serpentine, were detected in both indoor and outdoor dust samples. They are known by their anthropogenic character, namely as raw materials for magnesia refractories and construction. Chrysotile asbestos is the predominant commercial form of asbestos that has been used in insulation, roofing, vinyl floor tiles, heating appliances (such as clothes dryers and ovens), and ironing boards. Although it was phased out in many countries because of its health hazards, asbestos continues to be used in some products, such as brake pads and linings. The XRD patterns showed low crystallinity phases in small amounts (<5%), both in indoor and outdoor dust samples. Additionally, these mineral phases occur solely in a few samples. Halite was detected in two out of the 15 indoor dust samples, but in comparatively substantial amounts (9% and 13%).

3.2. Total Element Concentrations

Elemental concentrations determined in indoor and outdoor dust samples are summarised in Table S1 of the Electronic Supporting Information. The distribution pattern varied among elements. Significantly ($p < 0.01$) higher concentrations were observed for bismuth (Bi), boron (B), Cr, Cu, Cd, K, sodium (Na), Ni, Sb, tin (Sn), tungsten (W), and Hg in the indoor dust, and As, beryllium (Be), cesium (Cs), Fe, gallium (Ga), lithium (Li), manganese (Mn), rubidium (Rb), scandium (Sc), thorium (Th), thallium (Tl), uranium (U), vanadium (V), and yttrium (Y) in the outdoor dust. Differences between groups are not statistically significant ($p > 0.01$) for Al, barium (Ba), calcium (Ca), Co, Mg, molybdenum (Mo), Pb, selenium (Se), strontium (Sr), Zn, and zirconium (Zr). It is of note that, although the concentrations of Pb and Zn were more elevated in the indoor dust, the difference is not statistically significant. However, the values are higher than the ones reported for other cities around the world, as discussed in earlier studies by the authors [12,26]. Further, both PTEs show an anomalous enrichment in the household dust [26]. For those elements showing no significant differences between groups, only Zn shows a significant ($p < 0.05$) positive correlation (Spearman rho = 0.56) between indoor and outdoor dust samples, which indicates a possibly high contribution from exterior sources to the Zn indoor dust content. Zinc enriched windblown dust can enter through the windows and doors into the home environment.

To evaluate whether differences in the PTEs distribution produced a unique signature for indoor dust (IN) compared with outdoor dust (OUT), a stepwise MDA model was estimated comparing the indoor dust data to the outdoor dust data. Chemical elements with significantly higher contents in the indoor dust were the ones included in the analysis, as they were considered the most relevant to our exposure scenario. The number of discriminant functions estimated was one less than the number of groups being classified. The Wilks' lambda test ($p < 0.005$) and leave-one-out cross-validation were the methods used to evaluate the ability of the stepwise MDA model to classify samples into the two dust categories. Table 2 presents the sample classification matrix for the stepwise MDA model. The rows show the actual classification of the samples and the columns show the classifications given by the MDA model. Further information on the stepwise MDA model is provided in the Electronic Supporting Information (Table S2). The variables Na, K, Cd and Sn were the most important in the separation of the two groups. From Table 2, only one outdoor dust sample was misclassified as indoor dust. The MDA model classified with accuracy the dust samples, with a proportion of indoor dust

samples classified as indoor (sensitivity) of 100% and a proportion of outdoor samples classified as outdoor (specificity) of 94%, based on the leave-one-out classification matrix.

Overall, the results suggested distinct chemistry for indoor and outdoor dust samples, with significantly higher concentrations of Bi, B, Cr, Cu, Cd, K, Na, Ni, Sb, Sn, W, and Hg in the indoor dust. Cadmium, K, Na, and Sn seem to be important in the distinct chemistry of the indoor dust (Table S2). Reis and co-authors suggested mixed anthropogenic sources with contributions from sea salts and mineral dust/soil, as probable sources of these elements in the indoor dust samples [12].

Table 2. Sample classification matrix for the stepwise multiple discriminant analysis (MDA) obtained for the dust chemistry.

	Indoor Dust	Outdoor Dust	Total
Indoor dust	19	0	19
Outdoor dust	1	17	18

Like other PTEs, Pb and Zn showed higher concentrations in the indoor dust that are not, however, statistically significant. The positive correlation between indoor and outdoor samples found for Zn concentrations suggests an exterior contribution to the Zn dust contents indoor.

3.3. Solid-Phase Distribution of the Elements in the Indoor Dust

The solid-phase distribution of elements thought to be relevant for interpretation purposes was investigated. Knowledge of the PTEs' solid-phase associations allows a better understanding of their solubility and mobility, therefore elucidating the influence of dust mineralogy on in vitro bioaccessibility. The CISED procedure uses aqua regia at increasing concentrations to solubilize the different dust phases. Following ICP-AES analysis of each acid extract for the determination of 30 chemical elements (Tables S3–S6), the SMMR algorithm was used to determine how many phases were dissolved and how much of each phase was dissolved by a particular acid strength [32,33].

The SMMR modelling identified seven separate physicochemical components for dust collected from sites #1, #2, and #8, and six components for site #12, which was a 50-year-old house that, at the time, was being restored. Hence, it was assumed that dust from site #12 might have a significant contribution from building materials such as concrete, debris from tiles, bricks and roof tiles, and paint scraps. Compositional similarities and an equal number of components obtained by the SMMR modelling were observed for sites #1, #2, and #8. As such, the dust extracts were processed as a group and then combined into a single input data for the SMMR analysis as described elsewhere [34]. For this group, the chemometric data analysis identified seven physicochemical components. The components were tentatively assigned to different solid phases (Table 3) using the information on indoor dust chemistry, the relative solubility of each component in the extracts, and their major element composition (Figures S2 and S3).

3.3.1. Water Soluble Salt Phase

For grouped extracts (from samples #1, #2, and #8), the water-soluble salt component (Table 3) was made up of Na (ca. 59.6%), S (ca. 19.3%), and K (ca. 15.1%). Calcium (ca. 3.2%) was the other element extracted in considerable amounts.

The water-soluble salt component of dust collected from site #12 was composed of Na (ca. 33.9%), K (ca. 31.3%), and S (ca. 29.2%). Other elements extracted were Mg (ca. 1.8%), and Zn (ca. 1.5%).

These constituents were predominantly extracted with water, which, associated with the proximity of the sea, suggests a potential contribution of salt particles from sea spray to the indoor dust composition. A considerable amount of Zn was extracted with water from the indoor dust, especially from sample 12IN (Figures S4a and S5a), that can easily be available for humans following ingestion. It has been established that cement and concrete contain PTEs [46], and therefore water-soluble Zn determined in sample 12IN likely relates to building materials.

Table 3. Tentative geochemical assignment of components identified in grouped and #12 extracts, by CISED. Composition refers to the component composition based on >10% elemental presence. The profile shows the major elemental composition of profiles.

Samples 1IN+2IN+8IN			
Component	**Composition**	**Geochemical Assignment**	**Profile**
1	Na-S-K	Water soluble	Ca
2	Ca-K-Na-Mg	Exchangeable	P, Si, Al
3	Ca	Carbonate	Mg, P
4	Al	Al-dominated	Fe, Zn, P
5	Ca-Si	Clay related	Al, Mg, Zn
6	Fe-Al	Fe oxy-hydroxides	Si-S
7	Fe	Fe oxides	Al, S
Sample 12IN			
Component	**Composition**	**Geochemical Assignment**	**Profile**
1	Na-K-S	Water soluble	Mg, Zn
2	Ca-Zn-K	Exchangeable	Mg, P
3	Ca	Carbonate I	Zn
4	Ca	Carbonate II	P, Si
5	Ca	Ca-dominated	Al, Fe, Zn
6	Fe-Al	Fe oxy-hydroxides	Si-S

3.3.2. Exchangeable Phase

Component 2 was identified as an exchangeable component (Table 3) and was composed of mainly Ca (ca. 37.7%), K (ca. 23.4%), Na (ca. 13.4%), and Mg (ca. 12.5%).

The exchangeable component composition in site #12 (sample 12IN) was slightly different, mainly comprising Ca (ca. 59.5%), Zn (ca. 15.1%), and K (ca. 13.1%). This component was extracted by water and acid extracts over the whole concentration range employed in the CISED (Figures S2 and S3), which is similar to CISED data reported in previous studies [30,47]. It is noteworthy that, in site #12, Zn was a major constituent of the exchangeable phase (Figure S5a), indicating high mobility for this PTE.

3.3.3. Carbonate Phase

For the grouped extracts, the carbonate component (Table 3) consisted of Ca (ca. 96.1%). High Ca concentrations associated with extraction by weak acid suggest that the component relates to the dissolution of a calcium carbonate phase [30,47].

In sample 12IN, two components were identified as carbonate phases. They were considered to be chemically distinct because of their different extraction profiles (Figure S3), the small differences in their composition, and the distinctly larger mass of carbonate I. This component consisted of Ca (ca. 93.3%) and minor amounts of Zn (ca. 5.2%), while carbonate II was made up of Ca (ca. 95.3%) and minor amounts of Si and P (ca. 1.2%). The components were extracted by weak to moderate acid solutions (0.05 M-0.5 M aqua regia), with carbonate II requiring a slightly higher acid concentration for its removal, appearing later in the extraction profile.

Substantial amounts of calcite were identified in the indoor dust samples by the XRD analysis (Table 1), indicating that these components were derived from calcium carbonate.

3.3.4. Ca-Dominated Phase

This component (Table 3) was found only for sample 12IN and consisted mainly of Ca (ca. 84.4%) and to a lesser extent of Al (ca. 4.5%), Zn (ca. 2.8%), and Fe (ca. 2.5%). The component also consisted of the highest percentage of Ni, Pb, and Cu (Figure S5b–d, respectively) released during moderate to high acid CISED extractions. Some authors indicate Ca as a typical soil component when associated to Si or Mg [15], which are indicative of a crustal source, while others suggest an association with the

wear of asphalt concrete or building materials [12,48–50]. At the time of dust collection, the house was being restored, and debris and building materials as concrete, plaster, and bricks were visible throughout the site, which, associated with the composition of the component, led us to interpret it as Ca-carbonates of anthropogenic origin. Since these are technogenic materials, the component was labelled Ca-dominated instead of Ca-carbonates, despite its carbonate composition.

3.3.5. Al-Dominated Phase

The Al-dominated component (Table 3) was composed of Al (ca. 57.5%) and, to a lesser extent of Fe (ca. 9.6%), Zn (ca. 9.5%), and P (ca. 7.7%). This component also consisted of the highest percentage of Ni, Pb, Cu, and Co (Figure S5b–e, respectively) released during moderate to acid concentrations (0.1–0.5 M aqua regia). The association between Al and Fe led us to identify this component as Al oxy-hydroxides. Al oxide is a weathering product of silicate minerals, including feldspars, which were identified by the XRD analysis (Table 1). Barrón and Torrent (2013) discussed the formation of 'gelatinous' or 'poorly crystalline Al hydroxide' from the weathering of Al-silicates. These gelatinous products are the precursors of more crystalline minerals (gibbsite or boehmite), the formation pathways of which depend on several factors, namely temperature, pH, concentration, and water activity [51]. Hence, the gibbsite identified by the XRD study may have been formed by such processes. Dust particles were shown to be enriched in P probably because of their high specific surface area that contributes to high P sorption capacity [52]. Moreover, studies on phosphorous speciation in dust have shown iron and aluminium-bound P [53]. Therefore, the association of Al with Fe and P is not entirely uncommon.

Aluminium oxy-hydroxides can adsorb PTEs in a specific manner, which testifies to their unquestionable role on bioavailability and mobility of metals and metalloids [51,54,55]. In this study, the Al-dominated component, not found in sample 12IN, seems to be an important phase controlling the mobility of the PTEs in the indoor dust.

3.3.6. Clay Related Phase

The clay related component (Table 3) was extracted only in the group comprising samples 1IN, 2IN and 8IN, and was composed of mainly Ca (ca. 69.6%) and Si (ca. 13.1%). Other elements extracted were Mg (ca. 4.0%), Al (ca. 3.7%) and Zn (ca. 3.1%). The wide extraction window (0.05 M–1.0 M), the compositional assemblage of Ca, Si, Al, and Mg, along with the presence of trace elements suggests this component is likely to be related to clay minerals in the dust. Although Zn components in soils have been extensively studied [56–59], lesser attention has been devoted to the element's distribution in house dust [11,60], and no studies were found reporting on Zn containing clays in house dust. Yet, it has been demonstrated that in soil, Zn has no particular bearing phases, but it can be fixed by penetrating the lattice portion of the clay minerals [61,62]. Further investigation would be useful, using spectroscopic methods such as scanning electron microscopy (SEM) or extended x-ray absorption fine structure spectroscopy (EXAFS), to confirm the existence of Zn-containing clay minerals in the indoor dust.

3.3.7. Fe Oxy-Hydroxides

For the grouped extracts, the Fe oxy-hydroxides component (Table 3) was made up of Fe (ca. 44.7%) and Al (ca. 12.1%). Other elements extracted were Si (ca. 9.7%) and S (ca. 2.6%), as well as minor amounts of PTEs such as Pb, Cu, Cr (Figure S4c,d,f, respectively).

In sample 12IN, this component consisted mainly of Fe (ca. 62.0%) and Al (ca. 12.7%) and to a lesser extent Si (ca. 7.8%) and S (ca. 4.3%). As it has a reasonably well-defined extraction window at medium to high acid strength, this component is probably Fe oxy-hydroxides, which are known to have a variable composition and are usually contaminated by a variety of elements.

3.3.8. Fe-Oxide

The Fe-oxide component (Table 3) was dissolved at a high acid concentration (5 M) and was not observed for sample 12IN. It was composed mainly of Fe (ca. 76.6%) and minor amounts of Al (ca. 9.0%) and S (ca. 2.0%). This component also consisted of the highest percentage of Cr, As, Sb, and Sn (Figure S4f–i, respectively), released during high acid CISED extractions.

The presence of two different Fe containing components suggests the existence of distinct Fe-oxide forms that were dissolved at different rates [30,32]. Here, the Fe containing components were identified as Fe oxy-hydroxides and Fe-oxides, with the later as the least soluble dust phase from the seven obtained by the SMMR modelling. The lower solubility indicates that the Fe-oxides component was more crystalline.

Elevated As contents in contaminated media such as soils and groundwater were earlier reported for the region of Estarreja [63,64]. In this study, As was extracted mainly associated with the more resistant components (Fe oxy-hydroxides/Fe-oxides) which, is in good agreement with earlier findings of the authors [12,26] that point towards crustal sources for the element. Substantial amounts of Zn were extracted with the first three CISED solutions, indicating high mobility for the PTE. Overall, the solid-phase distribution of the elements in the indoor dust suggests that dust collected from sites #1, #2, and #8 probably had a considerable contribution from outdoor dust entering the home environment, as indicated by the Al oxy-hydroxides component formed by weathering of Al-silicates. This component had the highest concentrations of Zn, Ni, Pb, Cu, and Co (Figure S4). This indicates that tracked-in soil by human movement acts as a source and sink of contaminants found inside the home. Sample 12IN (site #12) was composed mainly of Ca carbonate materials that, in part, may have derived from anthropogenic/technogenic materials used in the house renovation.

### 3.4. The Oral Bioaccessibility of PTEs in Indoor Dust Samples

Following the analysis of the total concentration of PTE in the <150 μm particle size fraction, a total of nine indoor dust samples were selected for the in vitro measurement of bioaccessible concentrations. The bioaccessible fraction (BAF) was calculated as:

$$BAF = \frac{UBM\ extracted\ element\ concentration\ in\ the\ stomach\ phase}{total\ element\ concentration} \times 100\%. \qquad (4)$$

The bioaccessible concentrations were measured in both the stomach and intestine phases of the UBM. Higher concentrations were seen in the stomach compared to the intestine phase for the majority of the elements. Hence, data obtained from the stomach phase were used as predictors of bioavailability. Earlier studies available from the literature concluded that a simple stomach-alone extraction provides a conservative and cost-effective approach for estimating the oral bioaccessibility of metals in the solid phase [36,65–67].

The bioaccessible concentrations and BAF of Cd, Co, Cr, Cu, Ni, Pb, and Zn, in the <150 μm size fractions of the indoor dust, are presented in Table S7. For the PTE understudy, the % bioaccessibility varied within a wide range of values. According to their mean values (Table S7), the BAF (%) of PTEs in the stomach phase of the UBM procedure increased in the order (Figure 1): Sb (13%) < Cr (22%) < Cu (30%) < Co (38%) ≈ Ni (40%) < Pb (60%) < Cd (81%) ≈ Zn (84%).

Although As and Pb bioaccessibility in household dust is well documented in the literature, other PTEs such as Sb, Co, and V are less studied [68]. Nevertheless, a small number of studies were found reporting on bioaccessible concentrations of PTEs in household dust, estimated using different extraction procedures (Table 4). It is of note that no study was found on the oral bioaccessibility of Sb in indoor dust. In general, the different studies reported similar trends for the considered PTEs. While Zn and Cd exhibited high BAF values, other PTEs such as Co, Cr, Cu, and Ni showed low bioaccessibility in the household dust.
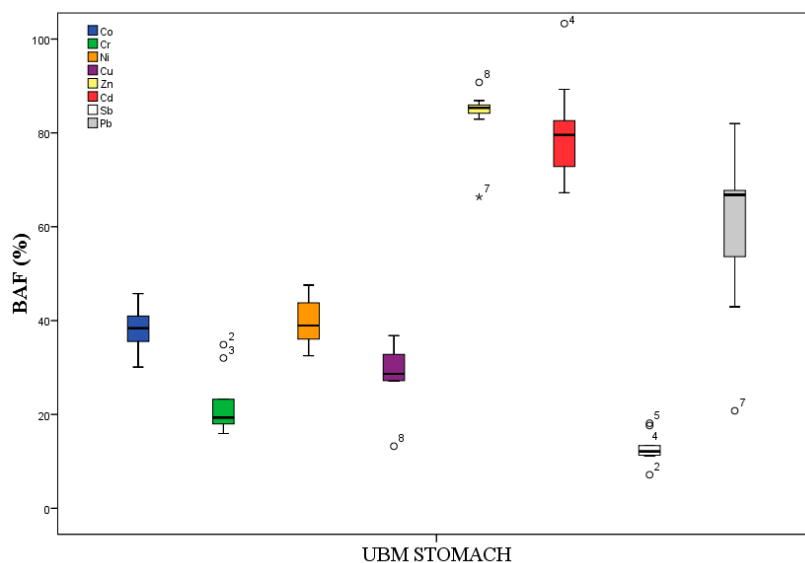
Figure 1. Box and Whisker plots showing the bioaccessible fraction of Co (blue), Cr (green), Ni (orange), Cu (purple), Zn (yellow), Cd (red), Sb (white), and Pb (gray color). Outlier values are indicated with circles or stars.

There is some consensus that solid-phase distribution is the main factor controlling the bioaccessibility of PTEs. For instance, higher bioaccessible fractions of Zn are usually associated with soluble Ca-minerals and, to a lesser extent, with Fe oxy-hydroxides [69,70]. Rasmussen et al. (2008) indicate a dominant role of the organic phase in controlling Cu accumulation in the household dust.

Table 4. Bioaccessibility of some potentially toxic elements (PTEs) in household settled dust samples.

Location	Extraction Procedure	PTE	BAF (%)	Study
Estarreja, Portugal	UBM: stomach phase	Co	38	This study
		Cr	22	
		Ni	40	
		Cu	30	
		Zn	84	
		Cd	81	
		Sb	13	
		Pb	60	
Plymouth, UK	Physiologically Based Extraction Technique (PBET): stomach phase	Cd	75	Turner & Ip (2007) [69]
		Co	15	
		Cr	10	
		Cu	15	
		Ni	20	
		Zn	80	
Ottawa, Canada	European Standard Toy Safety Protocol (EN-71 1995), modified	Cu	43	Rasmussen et al. (2008) [68]
		Ni	39	
		Zn	65	
Montreal, Canada	Physiologically Based Extraction Technique (PBET): stomach phase	Zn	77	Boros et al. (2017) [71]
		Pb	50	
		Cd	70	
		Cu	34	
		Ni	29	

To assess potential factors influencing the oral bioaccessibility, median CISED extracted PTE contents in samples #1, #2, and #8, and their average concentration extracted in the stomach phase of the UBM, were plotted simultaneously (Figure 2). Metal fractions associated with water-soluble,

exchangeable, and carbonates were extracted by the UBM solutions for the eight PTEs understudy. On the other end of the extraction sequence, metal fractions associated with more resistant dust components, e.g., clays and Fe oxides, were not extracted by the UBM solutions (Stomach = pH 1.2), indicating that these are not bioaccessible. For metal fractions associated with Al oxy-hydroxides, the results vary among the different PTEs. Substantial amounts of Cd (Figure 2b) and Pb (Figure 2c), and a significant proportion of Zn associated with this dust component, were extracted by the UBM procedure, rendering high %BAF (Table S7). Turner and Ip (2007) suggested that the majority of Zn in household dust is associated with Ca-bearing minerals that are readily solubilized in weak acid solutions. In our study, a significant fraction of bioaccessible Zn was also associated with Al-bearing phases. Copper, Ni, and Co were distributed differently with substantial amounts associated with Al oxy-hydroxides that are not extracted by the UBM acid solutions. As expected, these PTEs showed low %BAF. In the household dust, Sb and Cr were associated with more resistant Fe-bearing components (Figures S4 and S5), highlighted by the low bioaccessibility values obtained in the high acid (pH = 1.2) UBM stomach extraction.

Given the distinctive solid-phase distribution obtained for sample #12 (Figure S3), the data integration was performed by plotting median CISED extracted PTE and their concentration extracted in the stomach phase of the UBM (Figure 3), for this sample alone.

The striking feature is that in a carbonate matrix such as the one of sample 12 (Figure S3), except the Fe-oxide phase, all components were dissolved by the UBM solutions. This extensive dissolution had the greatest impact on Zn (Figure 3a), Cd (Figure 3b), Pb (Figure 3b), and Co (Figure 3f) bioaccessibility. As was earlier observed for sample group #1, #2, and #8, Cu, and to a lesser extent Ni, associated with the Ca-dominated component that was interpreted as an anthropogenic phase related to building materials, was not extracted by the UBM solutions. Hence, it is reasonable to assume that the solid-phase distribution was not the only factor influencing the oral bioaccessibility of the PTEs. It has been demonstrated that, unlike Zn that forms low stability complexes, Cu and Ni form stable complexes with pepsin as well as Cu-amino acid complexes, in the extracts of food supplements after in vitro simulation of gastric and gastrointestinal digestion [72].Therefore, it is possible that Cu and Ni extracted from dust by the UBM solutions formed complexes with pepsin in the gastric solutions which were not identified in the ICP-MS analysis, resulting in lower BAF values. The different complexes formed have different solubility and bioavailability, which has an impact on exposure and risk assessment. High Pb bioaccessibility has been determined when a solution containing 10 g·L^{-1} glycine, pepsin, or mucin, was applied to a soil [73], suggesting that the PTE forms low stability complexes with the gastric fluid constituents. In this study, major fractions of Pb, associated either with Al oxy-hydroxide or Ca-carbonate, were extracted by the UBM solutions, apparently without significant interference of the components used in the gastric fluids. Although the roles of some reagents such as glycine, pepsin, mucin, and citrate in controlling dissolution and precipitation of PTEs such as As, Pb, and Cd have been studied [73–75], the influence of these and other components on the bioaccessibility of these and other PTEs needs further investigation.

In this study, the number of samples used to estimate the bioaccessibility of the PTEs was small, and therefore, the values used may not be representative of the entire group. The limited number of samples hindered the use of a simple linear regression model for predicting bioaccessible concentrations of PTE. These factors are both limitations of the present study, however, the conclusions drawn from the present study were in good agreement with oral bioaccessibility studies conducted elsewhere [69–71].
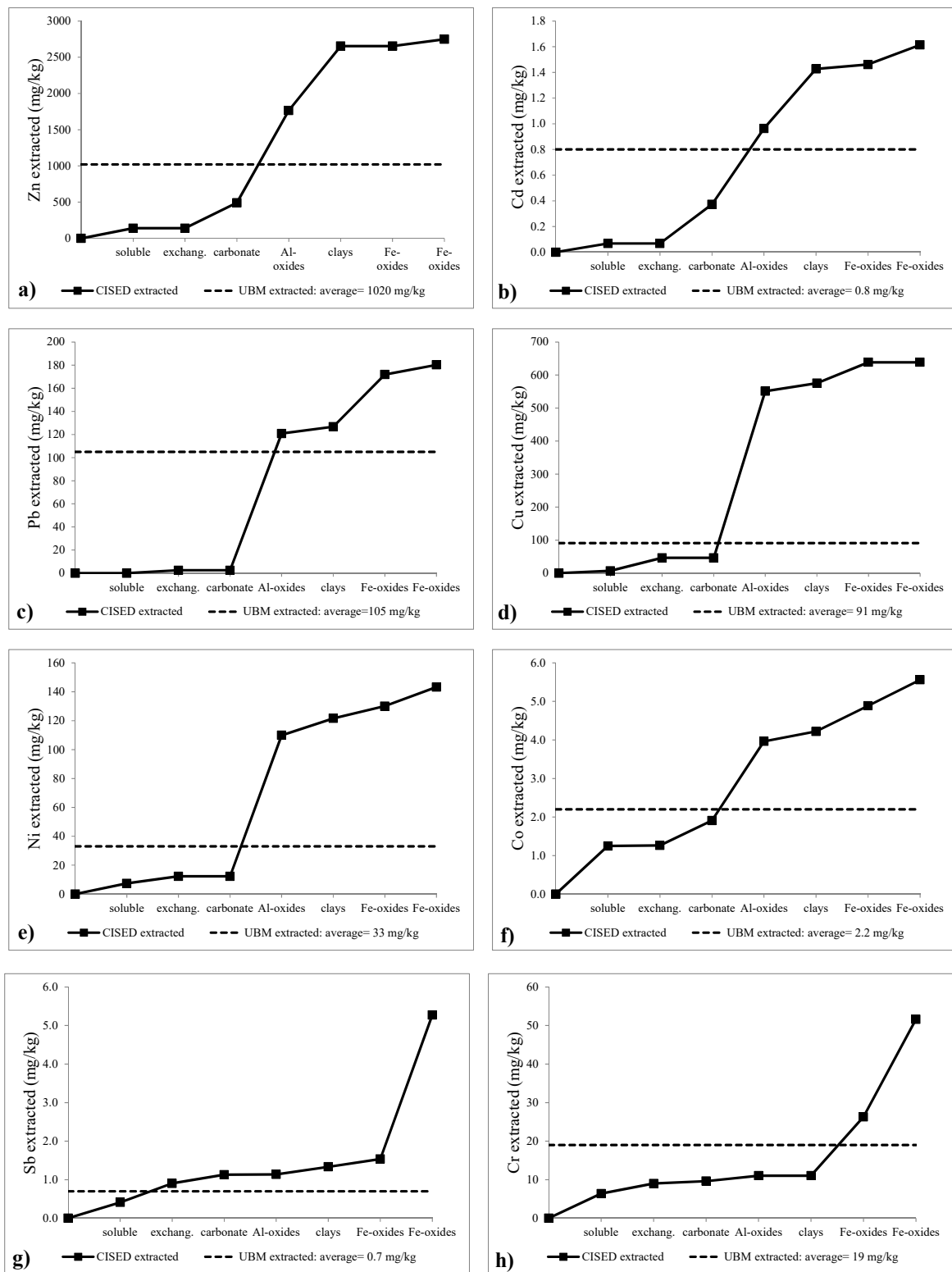
Figure 2. Median cumulative concentration in CISED extracted components (X-axis) and average bioaccessible concentration of Zn (**a**), Cd (**b**), Pb (**c**), Cu (**d**), Ni (**e**), Co (**f**) Sb (**g**), and Cr (**h**) (mg/kg) in sample group #1, #2 and #8. CISED extracted components are water soluble salt, exchangeable, Ca-carbonate, Al oxy-hydroxides, clays related, Fe oxy-hydroxides, and Fe-oxides.
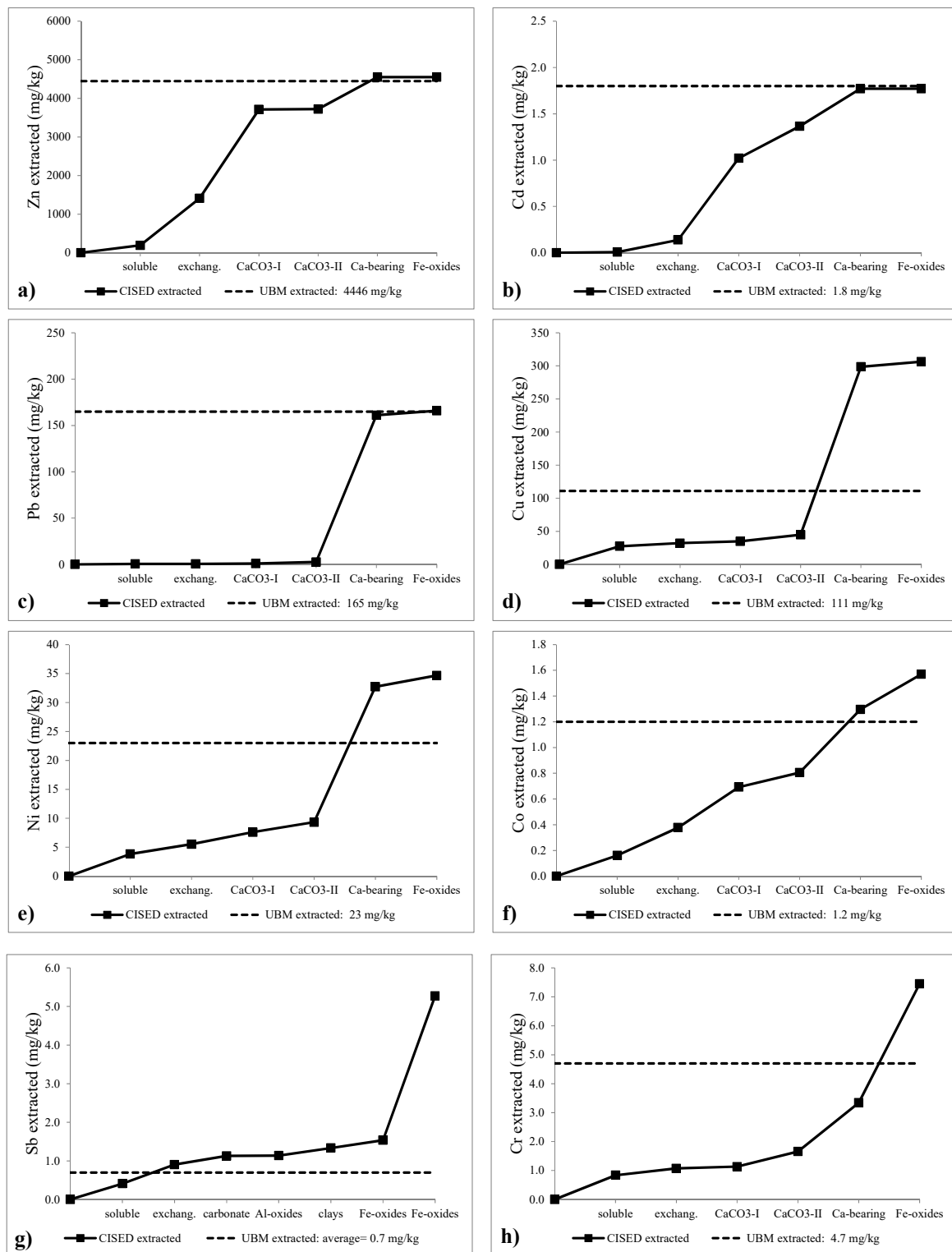
Figure 3. Median cumulative concentration in CISED extracted components (*X*-axis) and bioaccessible concentration of Zn (**a**), Cd (**b**), Pb (**c**), Cu (**d**), Ni (**e**), Co (**f**) Sb (**g**), and Cr (**h**) (mg/kg) in sample #12. CISED extracted components are water soluble salt, exchangeable, Ca-carbonate I, Ca-carbonate II, Ca-dominated, and Fe-oxides.

3.5. Human Health Risk Assessment for Indoor Dust Ingestion

The calculations for the ADD (Table S8) are based on several parameters; the uncertainty associated with the use of these variables has possibly resulted in an overestimation of the non- carcinogenic risk posed by the ingestion of the PTEs assessed in this study.

Only Pb had an HQ > 1 (Table 5), which indicates the risk of non-carcinogenic health effects, especially for children. Exposures to other individual PTEs are unlikely to pose a significant risk of non-carcinogenic effects based on the fact that the HQ values for the individual PTEs fell below the threshold value of 1. Lead excluded, Cu indicated greater contribution to the minimal risk of non-carcinogenic effects that may be observed among the children and the adult populations, followed by Co, Cr, and Zn. The higher HI values recorded for the child population (Table 5) suggest that children are more at risk of non-carcinogenic health effects following exposure to the dust in their home environment. Although the cumulative exposure to multiple toxic elements may not necessarily be additive, by this metric of assessment, it is clear that Pb is a major element for further consideration.

Table 5. Hazard quotient (HQ) and hazard index (HI) for Co, Cu, Pb, Sb, Cd, Cr, Ni, and Zn analysed in indoor dust of Estarreja households.

PTE	$HQ_{children}$	HQ_{adults}	$HI_{children}$	HI_{adults}
Co	0.45	0.20	-	-
Cu	0.51	0.22	-	-
Pb	3.39	1.47	-	-
Sb	0.15	0.06	-	-
Cd	0.05	0.02	-	-
Cr	0.34	0.15		
Ni	0.09	0.04		
Zn	0.25	0.11		
Σ	-	-	5.22	2.26

Inorganic Pb is a cumulative toxin absorbed mainly by the lungs and gastrointestinal tract. Lead exposure to children results in a significant decline in intellectual ability even at low-levels, with some studies indicating that the Pb associated intellectual decrement was steeper at low blood Pb levels than at higher blood Pb levels [76]. Additionally, this PTE is known to affect nearly every organ system in the body, including the nervous and cardiovascular systems [77,78]. Therefore, the impact of environmental exposure to Pb, even in low-levels, on the health of the public is substantial and primary prevention is pivotal as the consequences of lower blood Pb concentrations are recognized.

As observed earlier, indoor dust is an overlooked exposure pathway for PTEs in Portuguese homes. Although several uncertainties affect our health risk assessment output, from actual exposure frequency to the amount of contaminant available for contact by a person, the high HI values obtained both for children and adults urge the need for further investigation on this rather common exposure pathway.

4. Conclusions

This study provides insights on the biogeochemistry of selected PTEs (Co, Cr, Cu, Sb, Ni, Pb, and Zn) in 20 indoor dust samples from homes of a Portuguese industrial city, and their potential for causing chronic health effects in both adults and children.

Minor amounts of chrysotile, a hazardous material due to its asbestiform morphology, were detected in some samples, implying that further investigation may be warranted.

Multiple discriminant analysis showed that the chemistry of the dust discriminates well between indoor and outdoor samples. Potassium, Na, Cd and Sn, which showed significantly higher concentrations in the indoor dust, seem to be important in the discrimination.

Overall, the solid-phase distribution of the elements in indoor dust indicates that large proportions of Zn, Ni, Pb, Cu, and Co are associated with the Al oxy-hydroxides, formed by weathering of

Al-silicates, and released during moderate acid concentrations CISED extractions. This component, which seems to influence the mobility of many PTEs, was identified in a group of indoor dust samples that probably had a considerable contribution from windblown dust. Sample 12IN, collected from a house that was undergoing restoration, was composed mainly of Ca-carbonate materials that may have had an anthropogenic origin. The Fe-oxide component consisted of the highest percentage of Cr, As, Sb, and Sn, indicating low mobility for these elements.

The BAF in the stomach phase of the UBM procedure was generally high for Zn, Cd, and Pb (with Pb presenting broader variability), and low for Ni, Co, Cu, Cr, and Sb. Data integration with the solid-phase distribution provided a better understanding of the bioaccessibility measurements obtained by the UBM procedure. For the eight PTEs understudy, metal fractions associated with water-soluble, exchangeable, and carbonates were extracted by the UBM. As opposed, on the other end of the CISED extraction sequence, metal fractions associated with more resistant dust phases as clays and Fe oxides were not extracted by the UBM. However, in the more relevant metal-bearing components, Al oxy-hydroxides and Ca-carbonates, the PTEs show distinct behaviors. Most of the Cu and Ni associated with these components are not extracted by the UBM, probably because both PTEs form stable complexes with gastric fluid constituents such as pepsin and amino acids.

Lead had an HQ >1, which indicates the risk of non-carcinogenic health effects, especially for children, and the PTE is a major element for further consideration. Exposures to other individual PTEs pose no significant risk of non-carcinogenic effects.

Despite its uncertainties and limitations, this study provided relevant information about the pathways by which PTEs can be tracked into people's homes. Given the limited perception observed among the participants on potential health risks, from exposure to house dust, this study has highlighted the need to increase awareness of indoor dust as a common exposure pathway to environmental pollutants and provide information on how to reduce the tracking of PTEs from outdoors into the indoor environment.

References

1. World Health Organization (WHO). Burden of Disease from Household Air Pollution for 2016. Available online: https://www.who.int/airpollution/data/HAP_BoD_results_May2018_final.pdf (accessed on 30 March 2020).

2. Huang, M.; Wang, W.; Chan, C.Y.; Cheung, K.C.; Man, Y.B.; Wang, X.; Wong, M.H. Contamination and Risk Assessment (Based on Bioaccessibility via Ingestion and Inhalation) of Metal(Loid)s in Outdoor and Indoor Particles from Urban Centers of Guangzhou, China. *Sci. Total Environ.* **2014**, *479–480*, 117–124. [CrossRef] [PubMed]

3. Bari, A.; Kindzierski, W.B.; Wallace, L.A.; Wheeler, A.J.; Macneill, M.; Hèroux, M.-È. Indoor and Outdoor Levels and Sources of Submicron Particles (PM 1) at Homes in Edmonton, Canada. Environ. *Sci. Technol.* **2015**, *49*, 6419–6429. [CrossRef] [PubMed]

4. Madureira, J.; Paciência, I.; Rufo, J.; Ramos, E.; Barros, H.; Teixeira, J.P.; de Oliveira Fernandes, E. Indoor Air Quality in Schools and Its Relationship with Children's Respiratory Symptoms. *Atmos. Environ.* **2015**, *118*, 145–156. [CrossRef]

5. Tunno, B.J.; Dalton, R.; Cambal, L.; Holguin, F.; Lioy, P.; Clougherty, J.E. Indoor Source Apportionment in Urban Communities near Industrial Sites. *Atmos. Environ.* **2016**, *139*, 30–36. [CrossRef]

6. Jorquera, H.; Barraza, F.; Heyer, J.; Valdivia, G.; Schiappacasse, L.N.; Montoya, L.D. Indoor PM2.5 in an Urban Zone with Heavy Wood Smoke Pollution: The Case of Temuco, Chile. *Environ. Pollut.* **2018**, *236*, 477–487. [CrossRef]

7. Matawle, J.L.; Pervez, S.; Deb, M.K.; Shrivastava, A.; Tiwari, S. PM2.5 Pollution from Household Solid Fuel Burning Practices in Central India: 2. Application of Receptor Models for Source Apportionment. *Environ. Geochem. Health* **2018**, *40*, 145–161. [CrossRef]

8. Carrion-Matta, A.; Kang, C.M.; Gaffin, J.M.; Hauptman, M.; Phipatanakul, W.; Koutrakis, P.; Gold, D.R. Classroom Indoor PM2.5 Sources and Exposures in Inner-City Schools. *Environ. Int.* **2019**, *131*, 104968. [CrossRef]

9. Rivas, I.; Basagaña, X.; Cirach, M.; López-Vicente, M.; Suades-González, E.; Garcia-Esteban, R.; Álvarez-Pedrerol, M.; Dadvand, P.; Sunyer, J. Association between Early Life Exposure to Air Pollution and Working Memory and Attention. *Environ. Health Perspect.* **2019**, *127*. [CrossRef]

10. Gupta, P.; Satsangi, M.; Satsangi, G.P.; Jangid, A.; Liu, Y.; Pani, S.K.; Kumar, R. Exposure to Respirable and Fine Dust Particle over North-Central India: Chemical Characterization, Source Interpretation, and Health Risk Analysis. *Environ. Geochem. Health* **2020**, *42*, 2081–2099. [CrossRef]

11. Argyraki, A. Garden Soil and House Dust as Exposure Media for Lead Uptake in the Mining Village of Stratoni, Greece. *Environ. Geochem Health* **2014**, *36*, 677–692. [CrossRef]

12. Marinho Reis, A.P.; Cave, M.; Sousa, A.J.; Wragg, J.; Rangel, M.J.; Oliveira, A.R.; Patinha, C.; Rocha, F.; Orsiere, T.; Noack, Y. Lead and Zinc Concentrations in Household Dust and Toenails of the Residents (Estarreja, Portugal): A Source-Pathway-Fate Model. *Environ. Sci. Process. Impacts* **2018**, *20*, 1210–1224. [CrossRef]

13. Plumejeaud, S.; Reis, A.P.; Tassistro, V.; Patinha, C.; Noack, Y.; Orsière, T. Potentially Harmful Elements in House Dust from Estarreja, Portugal: Characterization and Genotoxicity of the Bioaccessible Fraction. *Environ. Geochem. Health* **2018**, *40*, 127–144. [CrossRef] [PubMed]

14. Hejami, A.A.; Davis, M.; Prete, D.; Lu, J.; Wang, S. Heavy Metals in Indoor Settled Dusts in Toronto, Canada. *Sci. Total Environ.* **2020**, *703*, 134895. [CrossRef]

15. Doyi, I.N.Y.; Isley, C.F.; Soltani, N.S.; Taylor, M.P. Human Exposure and Risk Associated with Trace Element Concentrations in Indoor Dust from Australian Homes. *Environ. Int.* **2019**, *133*, 105125. [CrossRef] [PubMed]

16. Miler, M.; Gosar, M. Assessment of Contribution of Metal Pollution Sources to Attic and Household Dust in Pb-Polluted Area. *Indoor Air* **2019**, *29*, 487–498. [CrossRef] [PubMed]

17. Fubini, B.; Fenoglio, I. Toxic Potential of Mineral Dusts. *Elements* **2007**, *3*, 407–414. [CrossRef]

18. Reis, A.P.; Patinha, C.; Wragg, J.; Dias, A.C.; Cave, M.; Sousa, A.J.; Batista, M.J.; Prazeres, C.; Costa, C.; Ferreira da Silva, E.; et al. Urban Geochemistry of Lead in Gardens, Playgrounds and Schoolyards of Lisbon, Portugal: Assessing Exposure and Risk to Human Health. *Appl. Geochem.* **2014**, *44*, 45–53. [CrossRef]

19. Candeias, C.; Da Silva, E.F.; Ávila, P.F.; Teixeira, J.P. Identifying Sources and Assessing Potential Risk of Exposure to Heavy Metals and Hazardous Materials in Mining Areas: The Case Study of Panasqueira Mine (Central Portugal) as an Example. *Geosciences* **2014**, *4*, 240–268. [CrossRef]

20. Reis, A.P.; Patinha, C.; Noack, Y.; Robert, S.; Dias, A.C.; Ferreira da Silva, E. Assessing the Human Health Risk for Aluminium, Zinc and Lead in Outdoor Dusts Collected in Recreational Sites Used by Children at an Industrial Area in the Western Part of the Bassin Minier de Provence, France. *J. Afr. Earth Sci.* **2014**, *99*, 724–734. [CrossRef]

21. Souza, E.D.; Texeira, R.; Cardoso da Costa, H.; Oliveira, F.; Melo, L.; Faial, K.; Fernandes, A. Assessment of Risk to Human Health from Simultaneous Exposure to Multiple Contaminants in an Artisanal Gold Mine in Serra Pelada, Pará, Brazil. *Sci. Total Environ.* **2017**, *576*, 683–695. [CrossRef]

22. Candeias, C.; Vicente, E.; Tomé, M.; Rocha, F.; Ávila, P.; Alves, C. Geochemical, Mineralogical and Morphological Characterisation of Road Dust and Associated Health Risks. *Int. J. Environ. Res. Public Health* **2020**, *17*, 1563. [CrossRef] [PubMed]

23. Comissão de Coordenação e Desenvolvimento Regional do Centro (CCDR). DATACENTRO. Informação para a Região. Available online: http://datacentro.ccdrc.pt/ (accessed on 21 October 2019).

24. Teixeira, C.; Assunção, C.F.T. *Mapa Geológico, Folha 13C*; Instituto Geográfico e Cadastral: Lisboa, Portugal, 1963. (In Portuguese)

25. Costa, C.; Jesus-Rydin, C. Site Investigation on Heavy Metals Contaminated Ground in Estarreja-Portugal. *Eng. Geol.* **2001**, *60*, 39–47. [CrossRef]

26. Reis, A.P.; Costa, S.; Santos, I.; Patinha, C.; Noack, Y.; Wragg, J.; Cave, M.; Sousa, A.J. Investigating Relationships between Biomarkers of Exposure and Environmental Copper and Manganese Levels in House Dusts from a Portuguese Industrial City. *Environ. Geochem. Health* **2015**, *37*, 725–744. [CrossRef]

27. Nowak, S.; Lafon, S.; Caquineau, S.; Journet, E.; Laurent, B. Quantitative Study of the Mineralogical Composition of Mineral Dust Aerosols by X-ray Diffraction. *Talanta* **2018**, *186*, 133–139. [CrossRef] [PubMed]

28. Shen, Z.; Caquineau, S.; Cao, J.; Zhang, X.; Han, Y.; Gaudichet, A.; Gomes, L. Mineralogical Characteristics of Soil Dust from Source Regions in Northern China. *Particuology* **2009**, *7*, 507–512. [CrossRef]

29. Denys, S.; Caboche, J.; Tack, K.; Rychen, G.; Wragg, J.; Cave, M.; Jondreville, C.; Feidt, C. In Vivo Validation of the UniFied BARGE Method to Assess the Bioaccessibility of Arsenic, Antimony, Cadmium, and Lead in Soils. *Environ. Sci. Technol.* **2012**, *46*, 6252–6260. [CrossRef]

30. Reis, A.P.; Patinha, C.; Wragg, J.; Dias, A.C.; Cave, M.; Sousa, A.J.; Costa, C.; Cachada, A.; Ferreira da Silva, E.; Rocha, F.; et al. Geochemistry, Mineralogy, Solid-Phase Fractionation and Oral Bioaccessibility of Lead in Urban Soils of Lisbon. *Environ. Geochem. Health* **2014**, *36*, 867–881. [CrossRef]

31. Ettler, V.; Štěpánek, D.; Mihaljevič, M.; Drahota, P.; Jedlicka, R.; Kříbek, B.; Vaněk, A.; Penížek, V.; Sracek, O.; Nyambe, I. Slag Dusts from Kabwe (Zambia): Contaminant Mineralogy and Oral Bioaccessibility. *Chemosphere* **2020**, *260*, 127642. [CrossRef]

32. Cave, M.R.; Milodowski, A.E.; Friel, E.N. Evaluation of a Method for Identification of Host Physico-Chemical Phases for Trace Metals and Measurement of Their Solid-Phase Partitioning in Soil Samples by Nitric Acid Extraction and Chemometric Mixture Resolution. *Geochem. Explor. Environ. Anal.* **2004**, *4*, 71–86. [CrossRef]

33. Cave, M.; Wragg, J.; Gowing, C.; Gardner, A. Measuring the Solid-Phase Fractionation of Lead in Urban and Rural Soils Using a Combination of Geochemical Survey Data and Chemical Extractions. *Environ. Geochem. Health* **2015**, *37*, 779–790. [CrossRef]

34. Amaibi, P.M.; Entwistle, J.A.; Kennedy, N.; Cave, M.; Kemp, S.J.; Potgieter-vermaak, S.; Dean, J.R. Mineralogy, Solid-Phase Fractionation and Chemical Extraction to Assess the Mobility and Availability of Arsenic in an Urban Environment. *Appl. Geochem.* **2019**, *100*, 244–257. [CrossRef]

35. Cave, M.R.; Rosende, M.; Mounteney, I.; Gardner, A.; Miró, M. New Insights into the Reliability of Automatic Dynamic Methods for Oral Bioaccessibility Testing: A Case Study for BGS102 Soil. *Environ. Sci. Technol.* **2016**, *50*, 9479–9486. [CrossRef] [PubMed]

36. Mehta, N.; Cocerva, T.; Cipullo, S.; Padoan, E.; Antonella, G.; Ajmone-marsan, F.; Fiona, S.; Coulon, F.; Antonio, D.; Luca, D. Linking Oral Bioaccessibility and Solid Phase Distribution of Potentially Toxic Elements in Extractive Waste and Soil from an Abandoned Mine Site: Case Study in Campello Monti, NW Italy. *Sci. Total Environ.* **2019**, *651*, 2799–2810. [CrossRef] [PubMed]

37. Carroll, S.; Goonetilleke, A.; Khalil, W.A.S.; Frost, R. Assessment via Discriminant Analysis of Soil Suitability for Effluent Renovation Using Undisturbed Soil Columns. *Geoderma* **2006**, *131*, 201–217. [CrossRef]

38. Scott, P.K.; Unice, K.M.; Williams, S.; Panko, J.M. Statistical Evaluation of Metal Concentrations as a Method for Identifying World Trade Center Dust in Buildings. *Environ. Forensics* **2007**, *8*, 301–311. [CrossRef]

39. Cabral Pinto, M.M.S.; Marinho-Reis, A.P.; Almeida, A.; Freitas, S.; Simões, M.R.; Diniz, M.L.; Pinto, E.; Ramos, P.; Ferreira da Silva, E.; Moreira, P.I. Fingernail Trace Element Content in Environmentally Exposed Individuals and Its Influence on Their Cognitive Status in Ageing. *Exposure Health* **2018**, *11*, 181–194. [CrossRef]

40. Johnston, R.J. *Multivariate Statistical Analysis in Geography: A Primer on the General Linear Model*, 1st ed.; Longman: New York, NY, USA, 1980; pp. 224–252.

41. US Environmental Protection Agency (US EPA). *Exposure Factors Handbook: 2011 Edition*; EPA/600/R-09/052F; National Center for Environmental Assessment: Washington, DC, USA, 2011. Available online: http://www.epa.gov/ncea/efh (accessed on 13 August 2020).

42. US Environmental Protection Agency (US EPA). *Guidelines for Exposure Assessment*; EPA/600/Z-92/001; National Center for Environmental Assessment: Washington, DC, USA, 1992. Available online: https://www.epa.gov/sites/production/files/2014-11/documents/guidelines_exp_assessment.pdf (accessed on 13 August 2020).

43. Antoine, J.M.R.; Fung, L.A.H.; Grant, C.N. Assessment of the Potential Health Risks Associated with the Aluminium, Arsenic, Cadmium and Lead Content in Selected Fruits and Vegetables Grown in Jamaica. *Toxicol. Rep.* **2017**, *4*, 181–187. [CrossRef]

44. US Environmental Protection Agency (US EPA). Provisional Peer Reviewed Toxicity Values for Cobalt (CASRN 7440-48-4). National Center for Environmental Assessment, Cincinnati, EPA/690/R-08/008F Final. Available online: https://cfpub.epa.gov/ncea/pprtv/documents/Cobalt.pdf (accessed on 24 August 2020).

45. Agency for Toxic Substances and Disease Registry (ASTDR). Toxicological Profile for Copper. U.S. Department of Health and Human Services. Available online: https://www.atsdr.cdc.gov/toxprofiles/tp132.pdf (accessed on 28 August 2020).

46. Bodaghpour, S.; Biglarijoo, N.; Ahmadi, S. A Review on the Existence of Chrome in Cement and Environmental Remedies to Control Its Effects. *Int. J. Geol.* **2012**, *6*, 62–67.

47. Wragg, J.; Cave, M. Assessment of a Geochemical Extraction Procedure to Determine the Solid Phase Fractionation and Bioaccessibility of Potentially Harmful Elements in Soils: A Case Study Using the NIST 2710 Reference Soil. *Anal. Chim. Acta* **2012**, *722*, 43–54. [CrossRef]

48. Kulshrestha, A.; Massey, D.D.; Masih, J.; Taneja, A. Source Characterization of Trace Elements in Indoor Environments at Urban, Rural and Roadside Sites in a Semi-Arid Region of India. *Aerosol Air Qual. Res.* **2014**, *14*, 1738–1751. [CrossRef]

49. Najmeddin, A.; Moore, F.; Keshavarzi, B.; Sadegh, Z. Pollution, Source Apportionment and Health Risk of Potentially Toxic Elements (PTEs) and Polycyclic Aromatic Hydrocarbons (PAHs) in Urban Street Dust of Mashhad, the Second Largest City of Iran. *J. Geochem. Explor.* **2018**, *190*, 154–169. [CrossRef]

50. Zannoni, D.; Valotto, G.; Visin, F.; Rampazzo, G. Sources and Distribution of Tracer Elements in Road Dust: The Venice Mainland Case of Study. *J. Geochem. Explor.* **2016**, *166*, 64–72. [CrossRef]

51. Barrón, V.; Torrent, J. Iron, Manganese and Aluminium Oxides and Oxyhydroxides. *Eur. Mineral. Union Notes Mineral.* **2013**, *14*, 297–336. [CrossRef]

52. Katra, I.; Gross, A.; Swet, N.; Tanner, S.; Krasnov, H.; Angert, A. Substantial Dust Loss of Bioavailable Phosphorus from Agricultural Soils. *Sci. Rep.* **2016**, *6*, 1–7. [CrossRef]

53. Gu, C.; Hart, S.C.; Turner, B.L.; Hu, Y.; Meng, Y.; Zhu, M. Aeolian Dust Deposition and the Perturbation of Phosphorus Transformations during Long-Term Ecosystem Development in a Cool, Semi-Arid Environment. *Geochim. Cosmochim. Acta* **2019**, *246*, 498–514. [CrossRef]

54. Goldberg, S.; Davis, J.A.; Hem, J.D. The surface chemistry of aluminium oxides and hydroxides. In *The Environmental Chemistry Aluminium*, 2nd ed.; Sposito, G., Ed.; CRC: Boca Raton, FL, USA, 1996; pp. 271–331.

55. Violante, A.; Cozzolino, V.; Perelomov, L.; Caporale, A.G.; Pigna, M. Mobility and Bioavailability of Heavy Metals and Metalloids in Soil Environments. *J. Soil Sci. Plant Nutr.* **2010**, *10*, 268–292. [CrossRef]

56. Scheinost, A.C.; Kretzschmar, R.; Pfister, S.; Roberts, D.R. Combining Selective Sequential Extractions, X-ray Absorption Spectroscopy, and Principal Component Analysis for Quantitative Zinc Speciation in Soil. *Environ. Sci. Technol.* **2002**, *36*, 5021–5028. [CrossRef] [PubMed]

57. Diesing, W.E.; Sinaj, S.; Sarret, G.; Manceau, A.; Flura, T.; Demaria, P.; Siegenthaler, A.; Sappin-Didier, V.; Frossard, E. Zinc Speciation and Isotopic Exchangeability in Soils Polluted with Heavy Metals. *Eur. J. Soil Sci.* **2008**, *59*, 716–729. [CrossRef]

58. Patinha, C.; Reis, A.P.; Dias, A.C.; Abduljelil, A.A.; Noack, Y.; Robert, S.; Cave, M.; Ferreira da Silva, E. The Mobility and Human Oral Bioaccessibility of Zn and Pb in Urban Dusts of Estarreja (N Portugal). *Environ. Geochem. Health* **2015**, *37*, 115–131. [CrossRef]

59. Kelepertzis, E.; Argyraki, A. Geochemical Associations for Evaluating the Availability of Potentially Harmful Elements in Urban Soils: Lessons Learnt from Athens, Greece. *Appl. Geochem.* **2015**, *59*, 63–73. [CrossRef]

60. Beauchemin, S.; Rasmussen, P.E.; Mackinnon, T.; Che, M.; Boros, K. Zinc in House Dust: Speciation, Bioaccessibility, and Impact of Humidity. *Environ. Sci. Technol.* **2014**, *48*, 9022–9029. [CrossRef] [PubMed]

61. White, M.L. The Occurrence of Zinc in Soil. *Econ. Geol.* **1957**, *52*, 645–651. [CrossRef]

62. Vodyanitskii, Y.N. Zinc Forms in Soils (Review of Publications). *Eurasian Soil Sci.* **2010**, *43*, 269–277. [CrossRef]

63. Inácio, M.; Neves, O.; Pereira, V.; Ferreira, E. Levels of Selected Potential Harmful Elements (PHEs) in Soils and Vegetables Used in Diet of the Population Living in the Surroundings of the Estarreja Chemical Complex (Portugal). *Appl. Geochem.* **2014**, *44*, 38–44. [CrossRef]

64. Cabral Pinto, M.M.S.; Marinho-Reis, A.P.; Almeida, A.; Ordens, C.M.; Silva, M.M.V.G.; Freitas, S.; Simões, M.R.; Moreira, P.I.; Dinis, P.A.; Diniz, M.L.; et al. Human Predisposition to Cognitive Impairment and Its Relation with Environmental Exposure to Potentially Toxic Elements. *Environ. Geochem. Health* **2018**, *40*, 1767–1784. [CrossRef]

65. Appleton, J.D.; Cave, M.R.; Palumbo-Roe, B.; Wragg, J. Lead Bioaccessibility in Topsoils from Lead Mineralisation and Urban Domains, UK. *Environ. Pollut.* **2013**, *178*, 278–287. [CrossRef]

66. Boisa, N.; Bird, G.; Brewer, P.A.; Dean, J.R.; Entwistle, J.A.; Kemp, S.J.; Macklin, M.G. Potentially Harmful Elements (PHEs) in Scalp Hair, Soil and Metallurgical Wastes in Mitrovica, Kosovo: The Role of Oral Bioaccessibility and Mineralogy in Human PHE Exposure. *Environ. Int.* **2013**, *60*, 56–70. [CrossRef]

67. Reis, A.P.; Patinha, C.; Noack, Y.; Robert, S.; Dias, A.C. Assessing Human Exposure to Aluminium, Chromium and Vanadium through Outdoor Dust Ingestion in the Bassin Minier de Provence, France. *Environ. Geochem. Health* **2014**, *36*, 303–317. [CrossRef]

68. Ibanez, Y.; Bot, B.; Le, G.P. House-Dust Metal Content and Bioaccessibility: A Review. *Eur. J. Miner.* **2010**, *22*, 629–637. [CrossRef]

69. Rasmussen, P.E.; Beauchemin, S.; Nugent, M.; Dugandzic, R.; Lanouette, M.; Chénier, M. Influence of Matrix Composition on the Bioaccessibility of Copper, Zinc, and Nickel in Urban Residential Dust and Soil. *Hum. Ecol. Risk Assess.* **2008**, *14*, 351–371. [CrossRef]

70. Turner, A.; Ip, K. Bioaccessibility of Metals in Dust from the Indoor Environment: Application of a Physiologically Based Extraction Test. *Environ. Sci. Technol.* **2007**, *41*, 7851–7856. [CrossRef] [PubMed]

71. Boros, K.; Fortin, D.; Jayawardene, I.; Chénier, M.; Levesque, C.; Rasmussen, P.E. Comparison of Gastric versus Gastrointestinal PBET Extractions for Estimating Oral Bioaccessibility of Metals in House Dust. *Int. J. Environ. Res. Public Health* **2017**, *14*, 92. [CrossRef] [PubMed]

72. Wojcieszek, J.; Witko, K.; Ruzik, L.; Pawlak, K. Comparison of Copper and Zinc in Vitro Bioaccessibility from Cyanobacteria Rich in Proteins and a Synthetic Supplement Containing Gluconate Complexes: LC–MS Mapping of Bioaccessible Copper Complexes. *Anal. Bioanal. Chem.* **2016**, *408*, 785–795. [CrossRef] [PubMed]

73. Li, J.; Li, K.; Cave, M.; Li, H.B.; Ma, L.Q. Lead Bioaccessibility in 12 Contaminated Soils from China: Correlation to Lead Relative Bioavailability and Lead in Different Fractions. *J. Hazard Mater.* **2015**, *295*, 55–62. [CrossRef]

74. Li, H.B.; Li, J.; Zhu, Y.G.; Juhasz, A.L.; Ma, L.Q. Comparison of Arsenic Bioaccessibility in Housedust and Contaminated Soils Based on Four in Vitro Assays. *Sci. Total Environ.* **2015**, *532*, 803–811. [CrossRef]

75. Li, H.; Li, M.; Zhao, D.; Li, J.; Li, S.; Xiang, P.; Juhasz, A.L.; Ma, L.Q.; Arsenic, L. Cadmium Bioaccessibility in Contaminated Soils: Measurements and Validations. *Crit. Rev. Environ. Sci. Technol.* **2020**, *50*, 1303–1338. [CrossRef]

76. Lanphear, B.P.; Hornung, R.; Khoury, J.; Yolton, K.; Baghurst, P.; Bellinger, D.C.; Canfield, R.L.; Dietrich, K.N.; Bornschein, R.; Greene, T.; et al. Low-Level Environmental Lead Exposure and Children's Intellectual Function: An International Pooled Analysis. *Environ. Health Perspect.* **2005**, *113*, 894–899. [CrossRef]

77. Caito, S.; Michael, A. Neurotoxicity of metals. In *Handbook of Clinical Neurology*; Marcello, L., Margit, L.B., Eds.; Elsevier: Amsterdam, The Netherlands, 2015; Volume 131, pp. 169–189. [CrossRef]

78. Nigra, A.E.; Ruiz-Hernandez, A.; Redon, J.; Navas-Acien, A.; Tellez-Plaza, M. Environmental Metals and Cardiovascular Disease in Adults: A Systematic Review beyond Lead and Cadmium. *Curr. Environ. Health Rep.* **2016**, *3*, 416–433. [CrossRef]